Research Article | Vol. 8, No. 4 | 1 Apr 2018 | OPTICAL MATERIALS EXPRESS 865
Optical Materials EXPRESS

Fabrication of Fe^{2+}:ZnSe nanocrystals and application for a passively Q-switched fiber laser

SHOUGUI NING,[1] GUOYING FENG,[1,3] HONG ZHANG,[1] WEI ZHANG,[1] SHENYU DAI,[1] YAO XIAO,[1] WEI LI,[1] XIAOXU CHEN,[1] AND SHOUHUAN ZHOU[1,2,4]

[1]*Institute of Laser &Micro/Nano Engineering, College of Electronics & Information Engineering, Sichuan University, No.24 South Section 1, Yihuan Road, Chengdu, Sichuan, 610064, China*
[2]*North China Research Institute of Electro-optics, Beijing, 100015, China*
[3]*guoing_feng@scu.edu.cn*
[4]*zhoush@scu.edu.cn*

Abstract: Fe^{2+}-doped ZnSe nanocrystals (NCs) were fabricated by femtosecond laser ablation in solution (FLAS). The synthesized Fe^{2+}:ZnSe NCs was characterized by XRD and SEM, which demonstrated the nanocrystalline characteristic of the sample. By spin-coating colloidal Fe^{2+}:ZnSe solution on a multiple-layer dielectric film, a Fe^{2+}:ZnSe saturable absorber (SA) was prepared. Employing the as-prepared Fe^{2+}:ZnSe NCs SA in an Er^{3+}:ZBLAN fiber laser, a passively Q-switched laser was successfully demonstrated at ~2.78 μm, with a recorded minimum pulse width of ~0.52 μs, maximum repetition rate of 127.46 kHz, peak power of 7.30 W and pulse energy of 3.81 μJ. This work shows Fe^{2+}:ZnSe NCs can be successfully fabricated by FLAS, and after ablation Fe^{2+}:ZnSe NCs can be efficient miniaturized SA device candidates for mid-IR fiber lasers and have great potential to be prepared on a fluoride fiber end for a compact all-fiber passively Q-switching laser at room temperature.

OCIS codes: (060.3510) Lasers, fiber; (140.3070) Infrared and far-infrared lasers; (140.3540) Laser, Q-switched; (160.3380) Laser material; (160.6990) Transmission-metal-doped material.

References and links

1. L. D. DeLoach, R. H. Page, G. D. Wilke, S. A. Payne, and W. F. Krupke, "Transition metal-doped zinc chalcogenides: spectroscopy and laser demonstration of a new class of gain media," IEEE J. Quantum Electron. **32**(6), 885–895 (1996).
2. R. H. Page, K. I. Schaffers, L. D. DeLoach, G. D. Wilke, F. D. Patel, J. B. Tassano, S. A. Payne, W. F. Krupke, K. T. Chen, and A. Burger, "Cr^{2+}-doped zinc chalcogenides as efficient, widely tunable mid-infrared lasers," IEEE J. Quantum Electron. **33**(4), 609–619 (1997).
3. S. Mirov, V. Fedorov, D. Martyshkin, I. Moskalev, M. Mirov, and V. Gapontsev, "Progress in mid-IR Cr^{2+} and Fe^{2+} doped II-VI materials and lasers [Invited]," Opt. Mater. Express **1**(5), 898–910 (2011).
4. S. Mirov, V. Fedorov, D. Martyshkin, I. Moskalev, M. Mirov, and S. Vasilyev, "Progress in Mid-IR Lasers Based on Cr and Fe Doped II-VI Chalcogenides," IEEE J. Sel. Top. Quantum Electron. **21**(1), 292–310 (2015).
5. J. J. Adams, C. Bibeau, R. H. Page, D. M. Krol, L. H. Furu, and S. A. Payne, "4.0-4.5-mum lasing of Fe:ZnSe below 180 K, a new mid-infrared laser material," Opt. Lett. **24**(23), 1720–1722 (1999).
6. J. Kernal, V. V. Fedorov, A. Gallian, S. B. Mirov, and V. V. Badikov, "3.9-4.8 μm gain-switched lasing of Fe:ZnSe at room temperature," Opt. Express **13**(26), 10608–10615 (2005).
7. S. D. Velikanov, N. A. Zaretskiy, E. A. Zotov, V. I. Kozlovsky, V. K. Yu, O. N. Krokhin, A. A. Maneshkin, P. P. Yu, S. A. Savinova, K. S. Ya, M. P. Frolov, R. S. Chuvatkin, and I. M. Yutkin, "Investigation of Fe:ZnSe laser in pulsed and repetitively pulsed regimes," Quantum Electron. **45**(1), 1–7 (2015).
8. A. A. Voronov, I. K. Vladimir, V. K. Yurii, I. L. Aleksandr, P. P. Yu, V. G. Polushkin, and M. P. Frolov, "Passive Fe^{2+}:ZnSe single-crystal Q switch for 3-μm lasers," Quantum Electron. **36**(1), 1–2 (2006).
9. X. Zhu, G. Zhu, C. Wei, L. V. Kotov, J. Wang, M. Tong, R. A. Norwood, and N. Peyghambarian, "Pulsed fluoride fiber lasers at 3 μm [Invited]," J. Opt. Soc. Am. B **34**(3), A15–A28 (2017).
10. J. Peppers, V. V. Fedorov, and S. B. Mirov, "Mid-IR photoluminescence of Fe^{2+} and Cr^{2+} ions in ZnSe crystal under excitation in charge transfer bands," Opt. Express **23**(4), 4406–4414 (2015).
11. C. Wei, H. Zhang, H. Shi, K. Konynenbelt, H. Luo, and Y. Liu, "Over 5-W Passively Q-Switched Mid-Infrared Fiber Laser With a Wide Continuous Wavelength Tuning Range," IEEE Photonics Technol. Lett. **29**(11), 881–884 (2017).

#319316 https://doi.org/10.1364/OME.8.000865
Journal © 2018 Received 9 Jan 2018; revised 23 Feb 2018; accepted 6 Mar 2018; published 12 Mar 2018

Optical Materials EXPRESS

12. C. Wei, X. Zhu, R. A. Norwood, and N. Peyghambarian, "Passively Q-Switched 2.8-μm Nanosecond Fiber Laser," IEEE Photonics Technol. Lett. **24**(19), 1741–1744 (2012).
13. G. Zhu, X. Zhu, K. Balakrishnan, R. A. Norwood, and N. Peyghambarian, "Fe^{2+}:ZnSe and graphene Q-switched singly Ho^{3+}-doped ZBLAN fiber lasers at 3 μm," Opt. Mater. Express **3**(9), 1365–1377 (2013).
14. Z. Tao, F. Guoying, Z. Hong, Y. Xianheng, D. Shenyu, and Z. Shouhuan, "2.78 μ m passively Q-switched Er^{3+}-doped ZBLAN fiber laser based on PLD-Fe^{2+}:ZnSe film," Laser Phys. Lett. **13**(7), 075102 (2016).
15. N. S. Myoung, V. V. Fedorov, and S. B. Mirov, "Optically dense Fe:ZnSe crystals for energy scaled gain switched lasing," Proceedings of SPIE - The International Society for Optical Engineering **7578**, 75781H–75781H–75788 (2010).
16. U. Demirbas, A. Sennaroglu, and M. Somer, "Synthesis and characterization of diffusion-doped Cr^{2+}:ZnSe and Fe^{2+}:ZnSe," Opt. Mater. **28**(3), 231–240 (2006).
17. L. Yang, J. Zhu, and D. Xiao, "Synthesis and characterization of ZnSe:Fe/ZnSe core/shell nanocrystals," J. Lumin. **148**, 129–133 (2014).
18. S. C. Erwin, L. Zu, M. I. Haftel, A. L. Efros, T. A. Kennedy, and D. J. Norris, "Doping semiconductor nanocrystals," Nature **436**(7047), 91–94 (2005).
19. N. Myoung, J. S. Park, A. Martinez, J. Peppers, S.-Y. Yim, W. S. Han, V. V. Fedorov, and S. B. Mirov, "Mid-IR spectroscopy of Fe:ZnSe quantum dots," Opt. Express **24**(5), 5366–5375 (2016).
20. G. Feng, C. Yang, and S. Zhou, "Nanocrystalline Cr^{2+}-doped ZnSe nanowires laser," Nano Lett. **13**(1), 272–275 (2013).
21. P. Russo, A. Hu, G. Compagnini, W. W. Duley, and N. Y. Zhou, "Femtosecond laser ablation of highly oriented pyrolytic graphite: a green route for large-scale production of porous graphene and graphene quantum dots," Nanoscale **6**(4), 2381–2389 (2014).
22. S. Barcikowski and G. Compagnini, "Advanced nanoparticle generation and excitation by lasers in liquids," Phys. Chem. Chem. Phys. **15**(9), 3022–3026 (2013).
23. P. P. Patil, D. M. Phase, S. A. Kulkarni, S. V. Ghaisas, S. K. Kulkarni, S. M. Kanetkar, S. B. Ogale, and V. G. Bhide, "Pulsed-laser-induced reactive quenching at liquid-solid interface: Aqueous oxidation of iron," Phys. Rev. Lett. **58**(3), 238–241 (1987).
24. S. B. Ogale, P. P. Patil, D. M. Phase, Y. V. Bhandarkar, S. K. Kulkarni, S. Kulkarni, S. V. Ghaisas, S. M. Kanetkar, V. G. Bhide, and S. Guha, "Synthesis of metastable phases via pulsed-laser-induced reactive quenching at liquid-solid interfaces," Phys. Rev. B Condens. Matter **36**(16), 8237–8250 (1987).
25. A. V. Kabashin, M. Meunier, C. Kingston, and J. H. T. Luong, "Fabrication and Characterization of Gold Nanoparticles by Femtosecond Laser Ablation in an Aqueous Solution of Cyclodextrins," J. Phys. Chem. B **107**(19), 4527–4531 (2003).
26. J.-P. Sylvestre, A. V. Kabashin, E. Sacher, and M. Meunier, "Femtosecond laser ablation of gold in water: influence of the laser-produced plasma on the nanoparticle size distribution," Appl. Phys., A Mater. Sci. Process. **80**(4), 753–758 (2005).
27. D. Tan, Z. Ma, B. Xu, Y. Dai, G. Ma, M. He, Z. Jin, and J. Qiu, "Surface passivated silicon nanocrystals with stable luminescence synthesized by femtosecond laser ablation in solution," Phys. Chem. Chem. Phys. **13**(45), 20255–20261 (2011).
28. M. E. Povarnitsyn, T. E. Itina, P. R. Levashov, and K. V. Khishchenko, "Mechanisms of nanoparticle formation by ultra-short laser ablation of metals in liquid environment," Phys. Chem. Chem. Phys. **15**(9), 3108–3114 (2013).
29. P. Blandin, K. A. Maximova, M. B. Gongalsky, J. F. Sanchez-Royo, V. S. Chirvony, M. Sentis, V. Y. Timoshenko, and A. V. Kabashin, "Femtosecond laser fragmentation from water-dispersed microcolloids: toward fast controllable growth of ultrapure Si-based nanomaterials for biological applications," J. Mater. Chem. B Mater. Biol. Med. **1**(19), 2489–2495 (2013).
30. D. Tan, B. Xu, P. Chen, Y. Dai, S. Zhou, G. Ma, and J. Qiu, "One-pot synthesis of luminescent hydrophilic silicon nanocrystals," RSC Advances **2**(22), 8254–8257 (2012).
31. T. Sakka, K. Saito, and Y. H. Ogata, "Confinement effect of laser ablation plume in liquids probed by self-absorption of C2 Swan band emission," J. Appl. Phys. **97**(1), 014902 (2005).
32. D. Tan, K. N. Sharafudeen, Y. Yue, and J. Qiu, "Femtosecond laser induced phenomena in transparent solid materials: Fundamentals and applications," PrMS **76**, 154–228 (2016).
33. A. Martinez, D. Martyshkin, R. Camata, V. Fedorov, and S. Mirov, "Crystal field engineering of transition metal doped II-VI ternary and quaternary semiconductors for mid-IR tunable laser applications," Opt. Mater. Express **5**(9), 2036–2046 (2015).
34. A. Martinez, L. Williams, V. Fedorov, and S. Mirov, "Gamma radiation-enhanced thermal diffusion of iron ions into II-VI semiconductor crystals," Opt. Mater. Express **5**(3), 558–565 (2015).
35. T. Zhang, G. Feng, H. Zhang, S. Ning, B. Lan, and S. Zhou, "Compact watt-level passively Q-switched ZrF_4-BaF_2-LaF_3-AlF_3-NaF fiber laser at 2.8 μm using Fe^{2+}:ZnSe saturable absorber mirror," Opt. Eng. **55**(8), 086106 (2016).
36. R. Herda, S. Kivistö, and O. G. Okhotnikov, "Dynamic gain induced pulse shortening in Q-switched lasers," Opt. Lett. **33**(9), 1011–1013 (2008).
37. J. Li, H. Luo, L. Wang, B. Zhai, H. Li, and Y. Liu, "Tunable Fe^{2+}:ZnSe passively Q-switched Ho^{3+}-doped ZBLAN fiber laser around 3 μm," Opt. Express **23**(17), 22362–22370 (2015).

Optical Materials EXPRESS

38. Z. Luo, D. Wu, B. Xu, H. Xu, Z. Cai, J. Peng, J. Weng, S. Xu, C. Zhu, F. Wang, Z. Sun, and H. Zhang, "Two-dimensional material-based saturable absorbers: towards compact visible-wavelength all-fiber pulsed lasers," Nanoscale **8**(2), 1066–1072 (2016).
39. C. Wei, X. Zhu, R. A. Norwood, and N. Peyghambarian, "Passively continuous-wave mode-locked Er^{3+}-doped ZBLAN fiber laser at 2.8 μm," Opt. Lett. **37**(18), 3849–3851 (2012).

1. Introduction

Recently, transition metal (TM) ions doped chalcogenide materials have attracted much interest in gain media for mid-infrared (mid-IR) lasers, which have extensive applications in spectroscopy, industrial processing, medical technology, environmental monitoring and biotechnology. TM ions doped chalcogenide materials were introduced to the laser community by Deloach [1] and Page [2] et al. Among the materials, Fe^{2+} doped ZnSe is one of the most important mid-IR materials both for the investigation of absorption and lasing in optoelectronic devices and lasers [3, 4]. The first tunable laser in 4.0-4.5 μm range using Fe^{2+}:ZnSe crystal has been demonstrated by Adams, J.J. et al. for temperature ranging from 15 to 180 K [5]. Afterwards, numerous studies have been published for the applications of Fe^{2+}:ZnSe crystal [4, 6, 7]. The significant breakthrough has been reported by S. Mirov et al. on the increasing average output power of Fe^{2+}:ZnSe crystal laser at liquid nitrogen temperature. The center wavelength was 4.15 μm with a polycrystal doped by diffusion method.

Apart from the application in mid-IR solid laser, Fe^{2+}:ZnSe is also a significant SA material for ~3 μm Q-switched fiber laser owing to the large absorptivity cross section, high damage threshold [8] as well as small-saturation fluence (~60 mJ/cm^2) [9]. The broad absorption band of Fe^{2+}:ZnSe crystal is corresponding to the $^5E \rightarrow {}^5T_2$ vibronic transmission of Fe^{2+} in the crystal field of ZnSe matrix, and this transmission ensures Fe^{2+}:ZnSe materials' application in passively Q-switched lasers [10, 11]. Fe^{2+}:ZnSe crystal served as SA and extensively applied in passive Q-switching mid-IR fiber lasers [8, 12, 13]. In order to avoid large inserting loss as well as constructing compact laser system with less optical components, Fe^{2+}:ZnSe film fabricated by pulse laser deposition (PLD), employed as a SA for Q-switched fiber laser has been reported [14]. For the sake of establishing all-fiber mid-IR laser, which has a more simple and compact structure, miniaturization of SA (Fe^{2+}:ZnSe) is of vital significance. One of the methods to promote fiber laser integration is to fabricate nanometer materials (NMs).

Thermo-diffusion method [15, 16] has been demonstrated a conventional way for preparing Fe^{2+}:ZnSe crystal, which was always employed as target for fabricating film or nanocrystals [14]. In addition, Fe:ZnSe nanocrystals have been reported to be synthesized by chemical routes [17], and the authors paid more attention to the application in visible spectral region. However, to apply in mid-IR spectral region, the existing organic molecule and high density of surface defects in the NCs fabricated via chemical means may result in the quenching of mid-IR luminescence [18, 19]. Whereas, femtosecond laser ablation (FLA), a physical process, has been proposed as a green method to synthesize various nanomaterials [20–22]. Owing to the typical ultra-short laser pulse width, which is shorter than the electron coupling time, therefore, the absorbed energy could be effectively injected into the materials and limited to the original focused volume, resulting in high efficiency target ablation. In 1987, Patil et al. [23,24] published their pioneering investigation on laser ablation of materials in solution, the possibility of synthesizing NCs by FLA in solution (FLAS) has stimulated extensive investigation attention. Afterwards, A.V.Kabashin et al. published their work that by FLAS in water and cyclodextrins solutions, Au nanoparticles were successfully fabricated [25, 26]. Since then, numerous studies were reported on the synthesis of NMs by using FLAS [27–30]. Compared to those ablation process in vacuum or gas phase, the solution in FLAS strongly confines the movement of species and plasma plume at the local point, which greatly influences the kinetic and thermodynamic characteristics of the transition of the plasma plume and products. Besides, FLAS can produce more extreme local thermodynamic conditions

with higher cooling rate, higher temperature and higher pressure than in vacuum or gases phase [31]. Thus, FLAS provides a convenient and clean technique for fabricating Fe^{2+}:ZnSe NCs. To our certain knowledge, this is the first demonstration of Fe:ZnSe nanocrystal preparation using the FLAS method.

In this paper, Fe^{2+}:ZnSe NCs were fabricated by FLAS. The XRD results demonstrated that the NCs' crystalline phase was in accordance with the bulk target material after ablation. Both are polycrystalline with a cubic zinc blende structure. The SEM characterization was performed on the fabricated NCs, giving an average size of ~90 nm. Finally, we demonstrated the practical application of the Fe^{2+}:ZnSe NCs as SA for a Q-switched mid-IR Er^{3+}-doped ZBLAN fiber laser. The Q-switched pulses have a pulse duration of ~520 ns, a repetition rate of ~127.46 kHz and a maximum output power of ~486 mW. The laser spectrum centers at ~2.78 μm with a FWHM of ~3 nm. This work demonstrated nanocrystalline Fe^{2+}:ZnSe can be efficient SAs for Er^{3+}:ZBLAN fiber laser and also implied the potential for application in compact all-fiber passively Q-switched ZBLAN laser.

2. Experimental

To fabricate Fe^{2+}:ZnSe NCs, ~0.5g micron Fe^{2+}:ZnSe powder was suspend in ~30 mL deionized water (DIW) in quartz bottle with a thickness of 1 mm. The micron Fe^{2+}:ZnSe powder was previously grinded from the Fe^{2+}:ZnSe bulk material, which was fabricated through vapor phase thermal diffusion means [20]. The dopant concentration of Fe^{2+} is calculated around ~3.93×10^{18} cm^{-3}. The observed Fe^{2+}:ZnSe NCs was fabricated by a commercial Ti:sapphire regenerate amplifier laser system (Legend Elite, Coherent). It generates ultrashort laser pulses (60 fs) and has a repetition rate of 1 kHz. The central wavelength is 800 nm. The average power is 1.4 W. The beam of laser was focused via a cylindrical lens (f = 10 cm) into the quartz vessel, which contain DIW suspended Fe^{2+}:ZnSe micron powder. Simultaneously, the dispersion was stirred via a magnetic stirrer with a constant speed of rotate (80 r/min). Prior to ablation, pure argon gas was bubbled into the suspension for about 2 hours to remove the dissolved oxygen. The whole ablation process was sustained for about 8 h. After the ablation process, the sample which suspend in DIW were precipitated by ethanol, washed with DIW and ethanol several times, the Fe^{2+}:ZnSe NCs were collected by centrifugation (10000 rpm, 10 min) and followed by dried at 35 °C for 2h in vacuum oven (~5×10^{-3} Pa). The schematic diagram of the FLAS experimental setup is shown in Fig. 1. The fabricated Fe^{2+}:ZnSe NCs' DIW dispersion solution can be seen in the upper inset in Fig. 1.

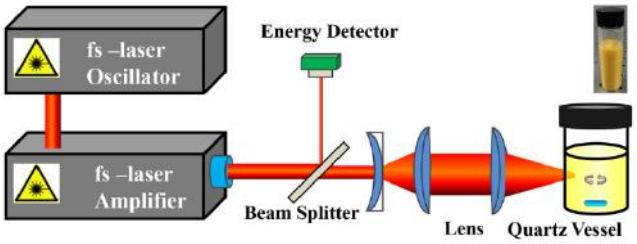

Fig. 1. The schematic diagram of the FLAS experimental setup. Inset: the photograph of Fe^{2+}:ZnSe NCs' DIW dispersion solution.

3. Discussion

To investigate the phase purity and crystalline properties of the Fe^{2+}:ZnSe NCs and target micrometer powder, X-ray powder diffraction (XRD) patterns were recorded on an X'pert Pro MPD (Philips Research) diffractometer with filtered 0.154 nm Cu Kα radiation. The XRD patterns of Fe^{2+}:ZnSe NCs and micron powder are presented in Fig. 2. The peaks of all the samples can be indexed as the cubic zinc blende structure, coincide with the standard PDF#

Optical Materials EXPRESS

37-1463. According to XRD results, Fe^{2+}:ZnSe NCs are polycrystalline after ablation by FLAS, in accordance with Fe^{2+}:ZnSe micron powder. The preferred orientation is along (111) planes with other most prominent planes of (220) and (311). The results indicated good crystallinity of Fe^{2+}:ZnSe NCs after ablation by FLAS.

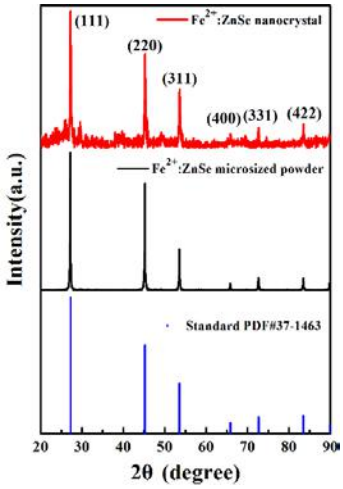

Fig. 2. XRD patterns of Fe^{2+}:ZnSe NCs and Fe^{2+}:ZnSe target micron powers.

Figure 3 (a) is the scan electron microscopy (SEM, Hitachi SU8220) image of the micron powders, Fig. 3(b) shows the SEM image of Fe^{2+}:ZnSe NCs, which are spherical in shape. The potential coalescence of the nanoparticles may increase the initial size of the NCs. Additionally, the ablation time and laser power may influence the resulted particles size [32]. To further observe the morphology of the NCs, we picked a larger single particle, the SEM image is seen in Fig. 3(c). The inset on the upper-right gives the photograph of diluted Fe^{2+}:ZnSe NCs solution used for SEM characterization. The statistical estimation of Fe^{2+}:ZnSe NCs size distribution is given in Fig. 3(d). The average particle size is ~90 nm, which indicates the nanocrystalline nature of the sample.

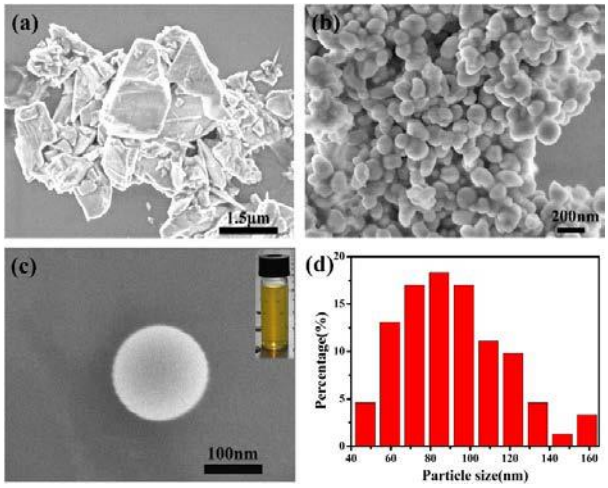

Fig. 3. SEM image of Fe^{2+}:ZnSe target micron powers (a), Fe^{2+}:ZnSe NCs (b) and (c), inset: the photograph of Fe^{2+}:ZnSe NCs solution for SEM characterization, particle size distribution of Fe^{2+}:ZnSe NCs (d).

Optical Materials EXPRESS

For estimating the thickness of the Fe^{2+}:ZnSe NCs coated on the dielectric film, the same amount of Fe^{2+}:ZnSe NCs solution was dropped on a sapphire substrate (with 20 mm diameter) in total, spin-coating and dried at room temperature. An atomic force microscopy (AFM, MFP-3D-BIO) was adopted. The surface profile of the Fe^{2+}:ZnSe NCs film is shown in Fig. 4(a), which implied that the NCs film was coalesced and stacked by NCs. The same aggregation phenomenon can also be seen in the SEM image in Fig. 3(b). Three positions (A, B and C) on the surface profile of the Fe^{2+}:ZnSe NCs film were selected and the height profiles were investigated along the red line, as shown in Fig. 4 (b),(c) and (d), respectively. The estimated average thickness of the NCs film is ~1.13 μm. It should be noted that the thickness of the film can be controlled by changing the concentration of Fe^{2+}:ZnSe NCs and the volume of the liquid solution that coated on the substrate. Certainly, the sample that employed for AFM characterization has the same concentration with that sample used for Q-switching.

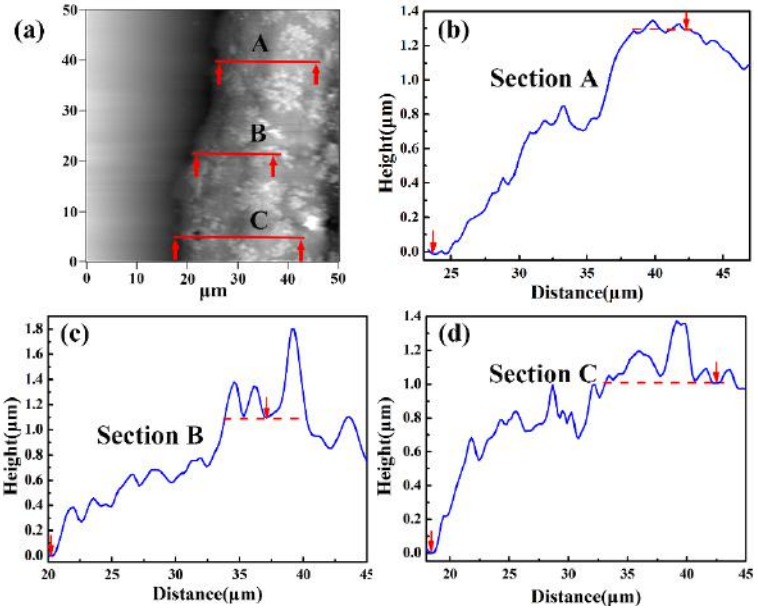

Fig. 4. (a) The surface profile of three typical position. (b), (c) and (d) The corresponding marked height curve of Fe^{2+}:ZnSe NCs on the sapphire substrate.

For measuring the optical absorption of Fe^{2+}:ZnSe NCs, the sample was measured with a Fourier Transform Infrared Spectrometer (Bruker, Tensor27). Figure 5(a) shows the corresponding linear transmission spectrum of sapphire substrate, Fe^{2+}:ZnSe NCs on the sapphire substrate and Fe^{2+}:ZnSe bulk material. Clearly, Fe^{2+}:ZnSe NCs has an absorption band between ~2.7-4.0 μm. However, for comparation with bulk material, the bulk Fe^{2+}:ZnSe (4 mm thick) have more broad absorption band in the range of ~2.3-4.5 μm [33, 34]. The existing Rayleigh scattering among the nanoparticles may result in the narrower absorption band. Furthermore, larger splitting happened between the excited triplet $^5T_2$ state and the ground state double ^5E states of Fe^{2+} in nanocrystalline environment may also cause the narrower absorption band. Because of the broad Mid-IR absorption as well as the large value of saturable cross-section, Fe^{2+}:ZnSe is regard as an excellent passively Q-switching element for Mid-IR fiber laser [12]. After fabrication, the Fe^{2+}:ZnSe NCs liquid solution was spin-coated onto a dielectric film with a diameter of 20 mm (the dielectric film was made up of ZnSe and CaF_2, alternately distributed on the sapphire substrate), and dried in air at room temperature to fabricate Fe^{2+}:ZnSe NCs SA. Figure 5(b) illustrates the linear transmission of the dielectric film and the Fe^{2+}:ZnSe NCs SA. The inset in Fig. 5(b) shows the photograph of

Optical Materials EXPRESS

the Fe^{2+}:ZnSe NCs SA. As seen, the transmission is less than 3% at 2.78 μm. Compared with the dielectric film, Fe^{2+}:ZnSe NCs SA on the dielectric film has lower transmission, due to scattering effect among Fe^{2+}:ZnSe NCs. Due to lack of suitable mid-IR pulse laser source with enough high peak power, the nonlinear absorption properties could not be measured, as reported in the ref [35].

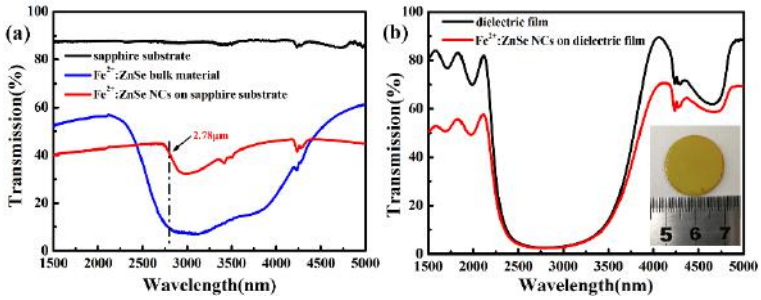

Fig. 5. (a) The transmission of sapphire substrate, Fe^{2+}:ZnSe NCs on sapphire substrate and ZnSe bulk material, (b) a multiple-layer dielectric film and Fe^{2+}:ZnSe NCs SA. Inset: the photograph of Fe^{2+}:ZnSe NCs SA.

For the purpose of demonstrating the practical application of the Fe^{2+}:ZnSe NCs, a linear cavity was adopted to satisfy passive Q-switched mid-IR Er^{3+}-doped ZBLAN fiber laser by using the Fe^{2+}:ZnSe NCs SA. The schematic diagram is shown in Fig. 6. The 976-nm laser diode was used as pump source, which has a maximum output power of 30W. Two plano-convex CaF_2 lenses (f = 35 mm) were employed to collimate and focus the pump laser into the inner cladding of the grain fiber. The dichroic mirror (DM), which has a >99% reflection at 2.8 μm and >98% transmission at 976 nm, was positioned between the CaF_2 lenses and placed at an angle 45° to output the laser beam. The employed gain fiber (Fiber Labs Inc.), with a total length of ~1.0 m, is a double-cladding Er^{3+} doped ZBLAN fiber. The diameter and NA of the core is 33 μm and 0.12, respectively. The diameter of the octagonal inner cladding is 330 μm with a NA of 0.5. The end facet of the grain fiber which close to the pump was vertically cleaved and was used as the output coupler mirror. The other end was cleaved at ~7° to eliminate the effect of parasitic oscillation. To reduce the unstable performance of the fiber laser induced by the thermal effects, a water-cooled fiber aluminum heatsink was used to fix the fiber and reduce the thermal damage of the pump end. The fabricated Fe^{2+}:ZnSe NCs SA was positioned closed to the fiber end to obtain Q-switching pulses. To remove background light, a long pass filter (>1.9 μm) was employed to purify the output laser and positioned in front of the detector. A thermal power meter (Coherent, PM10) was used to measure the average output laser power.

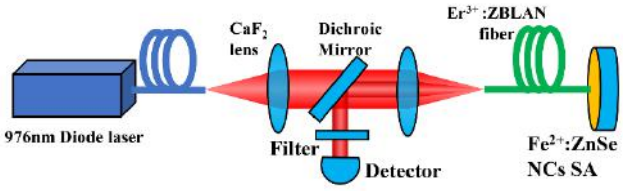

Fig. 6. Schematic diagram of the Q-switched Er^{3+}:ZBLAN fiber laser using Fe^{2+}:ZnSe NCs SA.

Figure 7 illustrates the Q-switched results with Fe^{2+}:ZnSe NCs SA. A HgCdTe detector (Vigo System S.A. model, PVI-3TE-5, ~20 ns response time) was used to record the pulse temporal waveform. In addition, a digital oscilloscope (Rohde & Schwarz, RTO1022, 2 GHz bandwidth) was used to record the pulses. The Q-switched pulse train, seen in Fig. 7(a), has a repetition rate of 91.59 kHz. With pump power increasing to 8.27 W, the repetition rate

Optical Materials EXPRESS

increased to 127.46 kHz. The corresponding pulse train is displayed in Fig. 7(b). Figure 7(c) shows the recorded single laser pulse, a Gaussian-like shape with FWHM of 2.66 μs and 0.52 μs with a pump power of 2.53 W and 8.27 W, respectively. The results are similar to the report in the ref [36], that grain compression effect under strong pumping resulted in the narrower pulses. The results are typical characteristics of passive Q-switching. This implied that Fe^{2+}:ZnSe NCs can indeed be employed for Q-switching in mid-IR fiber laser. Figure 7 (d) depicts the average output power versus pump power of the Q-switched fiber laser. With the increasing of pump power from 1.57 W to 8.27 W, the average output power linearly increased from 7.58 mW to 486 mW with a slope efficiency of 7.68%. The stable Q-switched pulses were first investigated as the pump power increased to 2.53 W. The recorded maximum average output power was 486 mW with a pump power of 8.27 W. The stable Q-switched operation could not be maintained if the incident pump power was continuously increased. It is likely that unstable Q-switching operation originated from the scattering effects. In addition, the output power was confined by the ~1 m gain fiber compared with our previous work, because of the reduced total gain. Nevertheless, further optimizing the output coupling ratio, increasing the pump coupling and increasing the Er^{3+} dopant concentration may contribute to increasing the output power [37, 38]. Furthermore, Fe^{2+}:ZnSe material has been reported to be used to generate mode-locked pulses with a pulse duration of 19 ps in Er^{3+}-doped ZBLAN fiber laser [39]. We suppose Fe^{2+}:ZnSe NCs have the potential to be employed for the generation of ultrafast mid-IR laser.

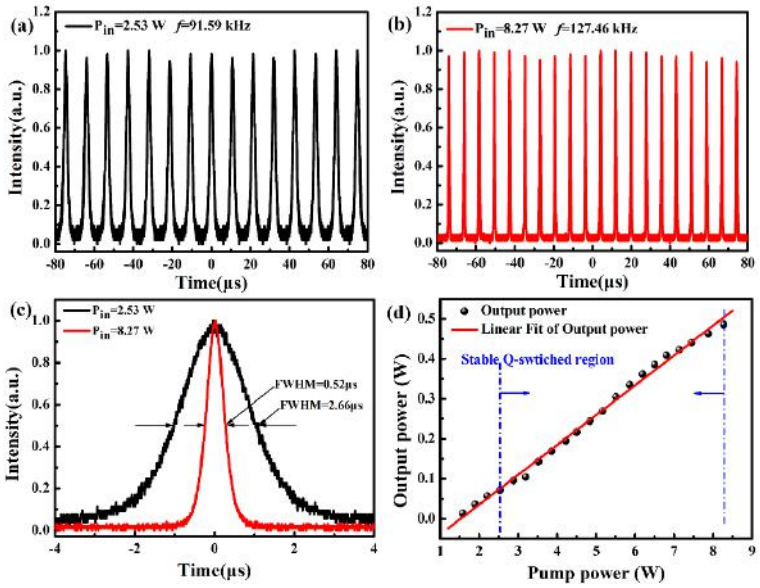

Fig. 7. The experimental results of the Fe^{2+}:ZnSe NCs Q-switched fiber laser. (a)Record pulse train at an incident pump power of 2.53 W, (b) record pulse train at an incident pump power of 8.27 W, (c) single pulse waveform, and (d) average output power as a function of incident pump power.

Figure 8(a) presents the laser optical spectrum of the Fe^{2+}:ZnSe NCs based fiber laser, which gives a central wavelength of ~2.78 μm and FWHM of ~3nm, corresponding to a typical $^4I_{11/2}$-$^4I_{13/2}$ transmission in an Er^{3+}-doped ZBLAN fiber laser. A monochromator (Princeton instruments Acton SP2750) was used to record the laser spectrum. Figure 8(b) and its inset give the RF spectrum of the Q-switched pulse train. With the pump power of ~8.27 W, the fundamental RF peak located at 127.46 kHz, with 150 kHz and a broad range of 2000 kHz span range, respectively. The signal-to-noise (SNR) is ~35 dB, indicating a good stability

Optical Materials EXPRESS

of the passively Q-switching operation, the result is similar to ref [13], which used Fe^{2+}:ZnSe bulk material as SA.

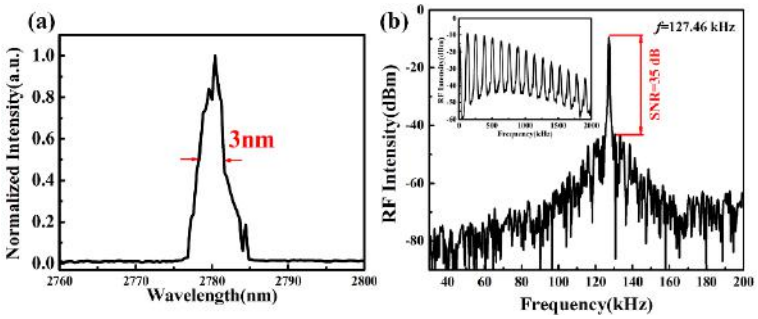

Fig. 8. (a) Output optical spectrum and (b) the SNR spectrum of the Fe^{2+}:ZnSe NCs based fiber laser. (Inset: the broad-band RF output spectrum.)

The pulse width and repetition rate of the Fe^{2+}:ZnSe NCs based fiber laser as a function of pump power are exhibited in Fig. 9(a). As can be seen, the pulse width decreased nonlinearly from 2.66 μs to 0.52 μs with the pump power changed from 2.53 W to 8.27 W. Moreover, the repetition rate increased from 91.59 kHz to 127.46 kHz due to the fast population built-up on $^4I_{11/2}$ level. Both of them are typical characteristics of passive Q-switching. The calculated pulse energy as well as peak power are depicted in Fig. 9(b). As expected, the pulse energy and peak power increased with the pump power increasing monotonously. A single pulse energy of 3.81 μJ and a peak power of 7.30 W was investigated with the incident pump power of 8.27 W. it is worth noting that high quality cleaved fiber end may contribute to gain much higher pulse energy and peak power. Additionally, much higher pulse energy can be obtained by using Fe^{2+}:ZnSe, because of its large damage threshold and optomechanical characteristics are superior to those other materials for Q-switching in mid-IR range [9].

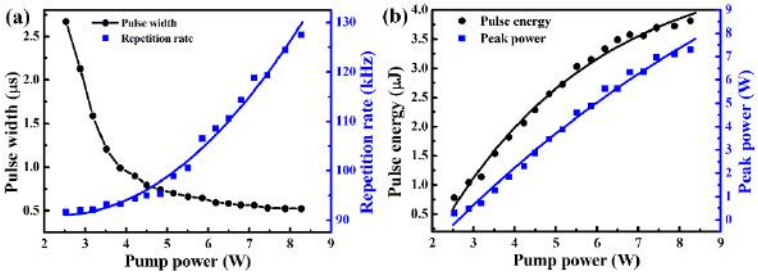

Fig. 9. (a) The repetition rate and pulse width versus incident pump power, (b) the power and single-pulse energy as a function of the incident pump power.

4. Conclusions

In conclusion, Fe^{2+}:ZnSe NCs were successfully fabricated by FLAS. The XRD and SEM characterization results demonstrated the good quality of Fe^{2+}:ZnSe NCs. Finally, we demonstrated the practical application of the Fe^{2+}:ZnSe NCs in a Q-switched mid-IR Er^{3+}-doped ZBLAN fiber laser. The Q-switched pulses have a pulse width of ~520 ns, a repetition rate of 127.46 kHz and a recorded maximum average output power of ~486 mW. The laser spectrum centered at ~2.78 μm with a ~3 nm FWHM. This work demonstrated Fe^{2+}:ZnSe NCs can be efficient SAs material for Er^{3+}:ZBLAN fiber laser and also implied the potential for fabricating miniaturized device on fluoride fiber end and application in compact all-fiber Q-switched fluoride lasers.

Optical Materials EXPRESS

Funding

National Natural Science Foundation of China. (NSFC No.11574221); the Joint Funds of the National Natural Science Foundation and the China Academy of Engineering Physics Foundation (NSAF, No. U1430126); National Natural Science Foundation of China for Youth (NSFC, No.11704268); Open Research Fund of Key Laboratory of High Energy Laser Science, CAEP (No.2013HEL05).